Identifying organic aerosol sources by comparing functional group composition in chamber and atmospheric particles

Lynn M. Russell[a,1], Ranjit Bahadur[a], and Paul J. Ziemann[b]

[a]Scripps Institution of Oceanography, University of California, San Diego, La Jolla, California; and [b]Air Pollution Research Center and Department of Chemistry, University of California, Riverside, California

Edited* by Mark H. Thiemens, University of California, San Diego, La Jolla, CA, and approved December 21, 2010 (received for review May 10, 2010)

Measurements of submicron particles by Fourier transform infrared spectroscopy in 14 campaigns in North America, Asia, South America, and Europe were used to identify characteristic organic functional group compositions of fuel combustion, terrestrial vegetation, and ocean bubble bursting sources, each of which often accounts for more than a third of organic mass (OM), and some of which is secondary organic aerosol (SOA) from gas-phase precursors. The majority of the OM consists of alkane, carboxylic acid, hydroxyl, and carbonyl groups. The organic functional groups formed from combustion and vegetation emissions are similar to the secondary products identified in chamber studies. The near absence of carbonyl groups in the observed SOA associated with combustion is consistent with alkane rather than aromatic precursors, and the absence of organonitrate groups can be explained by their hydrolysis in humid ambient conditions. The remote forest observations have ratios of carboxylic acid, organic hydroxyl, and nonacid carbonyl groups similar to those observed for isoprene and monoterpene chamber studies, but in biogenic aerosols transported downwind of urban areas the formation of esters replaces the acid and hydroxyl groups and leaves only nonacid carbonyl groups. The carbonyl groups in SOA associated with vegetation emissions provides striking evidence for the mechanism of esterification as the pathway for possible oligomerization reactions in the atmosphere. Forest fires include biogenic emissions that produce SOA with organic components similar to isoprene and monoterpene chamber studies, also resulting in nonacid carbonyl groups in SOA.

atmospheric aerosol | organic particles | smog chamber aerosol | alkane oxidation products | photochemical reactions

Recent literature reviews have highlighted significant advances in identifying compounds formed as "secondary" organic aerosol (SOA) in a wide range of laboratory-simulated atmospheric conditions, and field studies have identified several individual products from chamber studies (1–3). Paulot et al. have used global modeling to show that extrapolating these laboratory results for modeled global oxidant distributions helps explain biogenic SOA (4). However, the observations needed to confirm the proposed sources of organic aerosols (OAs) in global models—namely, quantitative field measurements of the proposed products to compare with the model predictions—remain elusive (5). Without such confirmation, it is difficult to identify which of the mechanisms proposed to explain controlled laboratory studies of simple volatile organic compound (VOC)-oxidant systems would satisfactorily capture those aspects of the chemistry that determine SOA formation in the more complex atmosphere.

There has been significant progress in quantifying organic mass (OM, the particle-phase components of OA) from the fragments produced by online mass spectrometry of particles, with recent promulgation of techniques to quantify the resulting mixtures by two to four fragment-based positive matrix factorization (PMF) factors: two types of oxidized, hydrocarbon-like, and biomass-burning OA. However, Donahue et al. (6) note that the traditional distinction between the directly emitted "primary" OA (POA) and the atmospherically formed SOA is difficult to define in atmospheric measurements. Similarly, the discrepancies between modeled and measured OM are difficult to resolve by comparisons of global budgets (5) without first verifying that the SOA formation pathways and yields employed in the global models are reflective of the real atmosphere. Definitions of modeled and measured POA and SOA are different, with models using inventories and yields based on controlled conditions and measurements using composition and correlations to infer a distinction. To overcome this disconnect, models can adjust yields to match observations. We propose to compare the measured organic functional group composition of atmospheric aerosols to those estimated from chamber studies to assess the extent to which their chemical similarity establishes the applicability of chamber measurements for predicting atmospheric SOA formation. Because functional groups have more chemical specificity than that in ion mass fragments or atomic oxygen-to-carbon (O/C) ratios, their relative contributions are valuable information to assess the possible SOA formation pathways in the atmosphere. In particular, we synthesize recent measurements of OM functional group composition from various field studies to identify which sources are associated with one or more oxygen-containing organic groups that were quantified in atmospheric aerosol by FTIR spectroscopy (carboxylic acid, carbonyl, hydroxyl, organosulfate, and organonitrate groups, with terms explained in *SI Text*). Although this approach does not identify individual molecular compounds that would serve as evidence of specific VOC reaction pathways, the quantification of major functional groups provides a constraint on the types of products that form in atmospheric conditions.

Results

The technique for measuring organic functional groups in atmospheric particles using FTIR is described in *SI Text*, with the measurements for the 21 projects listed in Table 1 and summarized in Fig. 1. The functional group composition has six notable trends: The first feature that is evident from this geographical overview is (*i*) the large contribution (often 50% of OM) of alkane groups in most campaigns, except in (*ii*) marine-dominated campaigns where hydroxyl groups contribute close to 50% of OM. The next clear trend is that (*iii*) the carboxylic acid group contribution accounts for 10 to 40% of OM in the 17 projects for which it was measured. An unexpected feature is the (*iv*) small

Author contributions: L.M.R. designed research; L.M.R. performed research; L.M.R. contributed new reagents/analytic tools; L.M.R., R.B., and P.J.Z. analyzed data; and L.M.R. and P.J.Z. wrote the paper.

The authors declare no conflict of interest.

*This Direct Submission article had a prearranged editor.

Freely available online through the PNAS open access option.

[1]To whom correspondence should be addressed. E-mail: lmrussell@ucsd.edu.

This article contains supporting information online at www.pnas.org/lookup/suppl/doi:10.1073/pnas.1006461108/-/DCSupplemental.

Table 1. Summary of 21 campaign OM and O/C measurements, with PMF factor characteristics identified for 12 separate PMF analyses of 1,368 spectra collected in 14 campaigns

			Fuel combustion[a]		Terrestrial vegetation		Ocean-biogenic	
Project	OM, $\mu g\,m^{-3}$	O/C (atomic)	O/C < 0.4	O/C > 0.4	Biogenic	Burning	O/C > 1	O/C < 1
PELTI, June 2000[b]								
NCAR C130 (St. Croix)	3.1	0.19						
ACE-Asia, April–May 2001[c]								
NCAR C130 (Iwakuni)	7.1	0.15						
R/V *Ronald Brown*	2.8	0.16						
New Jersey, August 2003[d]								
Princeton Fine Hall	2.6	0.15						
ICARTT, July–August 2004[e]								
TO: Twin Otter (Ohio)	5.5	0.61						
CP: Chebogue Point (Nova Scotia)	2.2	0.55						
AI: Appledore Island (Maine)	6.6	0.74						
RB: R/V *Ronald Brown* (Gulf of Maine)	4.7	0.43						
MILAGRO, March–April 2006[f]								
VC: NCAR C130 (Veracruz)	6.9	0.27						
MC: SIMAT (Mexico City)	9.5	0.45						
PD: Altzomoni (Paso de Cortez)	7.0	0.49						
ST: INTEX-B NCAR C130[g]								
Seattle, April–May 2006	2.4	0.37						
HO: TexAQS R/V *Ron Brown*[h]								
Houston, August–September 2006	4.9	0.46						
IC: ICEALOT R/V *Knorr*[i]								
Arctic, April–May 2008	0.64	0.88						
Scripps Pier[j]								
SP: June–August 2008	4.6	0.23						
SN, February–March 2009	1.6	0.57						
WH: Whistler Forest[k]								
May–June 2008	1.3	0.72						
VX: VOCALS, October–November 2008[l]								
R/V *Ronald Brown*	0.57	0.57						
BW: Barrow, Alaska[m]								
March–June2008	0.64	0.62						
July–October 2008	0.14	0.64						
November 2008–February 2009	0.51	1.2						
Products of Chamber Studies[n]								
C_{25} alkane, first generation								
C_{12} alkane, second generation								
Monoterpene								

Colors in pie charts indicate mass fraction of each organic functional group, showing alkane (blue), hydroxyl (pink), amine (orange), nonacid carbonyl (teal), carboxylic acid (green), organosulfate (yellow), and other (gray) group contributions. The three sizes of pie charts represent the average factor contribution range of <1 $\mu g\,m^{-3}$ (small), 1–3 $\mu g\,m^{-3}$ (medium), and >3 $\mu g\,m^{-3}$ (large). ACE-Asia, Asian Pacific Regional Aerosol Characterization Experiment.

[a]Fuel combustion includes fossil and other fuels associated with urban activities (16), and in Mexico City may also include emissions from incineration (14).
[b]Maria et al. (7).
[c]Maria et al. (8) and Quinn et al. (9).
[d]Maria and Russell (10).
[e]Gilardoni et al. (11) and Bahadur et al. (12).
[f]Gilardoni et al. (13) and Liu et al. (14).
[g]Day et al. (15).
[h]Russell et al. (16).
[i]Russell et al. (17).
[j]Hawkins and Russell (18) and Day et al. (19).
[k]Schwartz et al. (20).
[l]Hawkins et al. (21).
[m]Shaw et al. (22).
[n]This work, using alkane products derived from Lim and Ziemann (23, 24) and monoterpene products based on Capouet et al. (25).

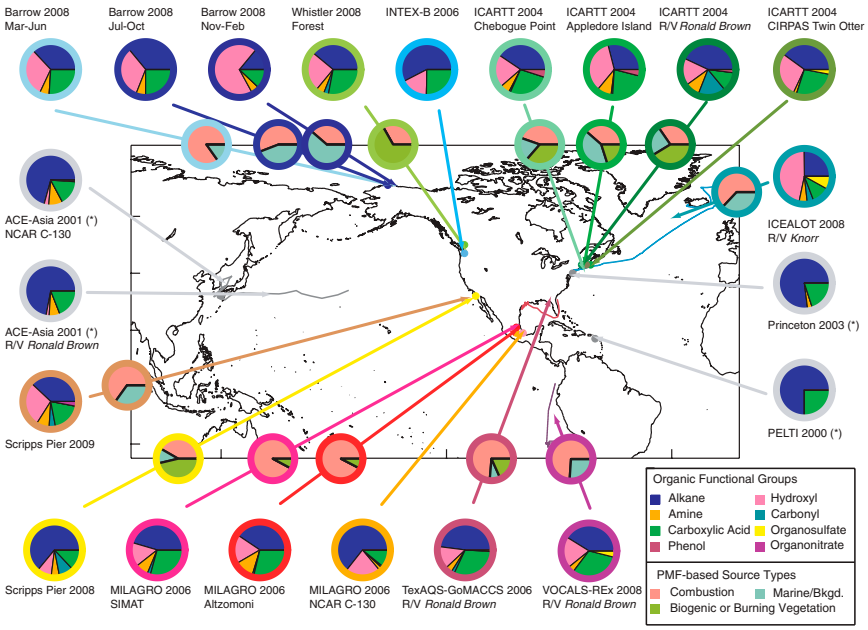

Fig. 1. Summary of mean organic functional group concentrations identified by FTIR for 21 field measurement campaigns during 2000–2009. Colors in organic functional group pie charts (outside the box) indicate mass fraction of each group, showing alkane (blue), hydroxyl (pink), amine (orange), nonacid carbonyl (teal), carboxylic acid (green), and organosulfate (yellow) group contributions; abbreviations for each campaign are described in Table 1. Colors in smaller pie charts on the arrows show factor contributions to each project, obtained from identifying PMF of FTIR spectra as factors associated with combustion (salmon), biogenic or biomass burning (jade), and marine (cerulean) (with factor compositions shown in Table 1 and factor spectra in Fig. 2). Arrows and outlines of pie charts are colored uniquely for each dataset, and this scheme is used in Fig. S1. Projects from 2000 to 2003 (indicated by an asterisk) show FTIR spectra measured with the Mattson Research Series 100 FTIR Spectrometer, and those from 2004 to 2009 were measured with the Bruker Tensor 27 FTIR Spectrometer. INTEX-B, Intercontinental Chemical Transport Experiment–Phase B; PELTI, Passing Efficiency of the Low Turbulence Inlet Experiment; SIMAT, Mexico City Atmospheric Monitoring System Building; NCAR C130, National Center for Atmospheric Research C130 Research Aircraft.

but consistent contribution of less than 10% of amine groups in all campaigns. Projects in three regions reveal (*v*) the occasional contribution of nonacid carbonyl groups associated with emissions from forested regions (both biogenic and biomass burning). Finally, (*vi*) several regions show less common organic functionality: Near high SO_2 emissions there are organosulfate groups, near high NO_x emissions there are organonitrate groups, and near densely forested areas there are phenol groups.

Preliminary hypotheses about the sources associated with each functional group type can be inferred from the types of emissions that dominate campaigns with the highest and most consistent contributions. The largest carboxylic acid group concentrations were identified with fuel combustion emissions for measurements in Houston and Mexico City, in which urban combustion sources are known to account for much of the fine particle mass. Two locations had substantial amounts of carbonyl groups: at a mid-mountain forested site in Whistler, British Columbia, Canada, and on the research vessel (R/V) *Ronald Brown* in the Gulf of Maine, suggesting an association between forest emissions and carbonyl groups that is consistent with the reported correlations of carbonyl-containing factors with biogenic VOCs in these projects (12, 20). The highest hydroxyl fractions were found over the Atlantic and Arctic Oceans [International Chemistry Experiment in the Arctic LOwer Troposphere (ICEALOT)] and in the more remote regions of the Southeastern Pacific Ocean [VAMOS Ocean-Cloud-Atmosphere-Land Study Regional Experiment (VOCALS-REx)], suggesting that these highly oxygenated organic components are associated with marine sources.

We apportioned organic functional groups to sources using PMF to identify recurring FTIR spectral features that were then associated with available emission tracers for each project (summarized in Table 1, cited references, and *SI Text*). Based on these correlations to emission tracers, each PMF factor in each project was assigned to a specific source type. Because of the multivariate nature of SOA formation in the atmosphere, the supporting measurements available for correlation on each campaign (provided in references cited in Table 1) include only a subset of tracers and typically reflect only mild correlations ($0.5 < r < 0.75$). However, the association of these factors with their most probable respective sources is significantly strengthened by the similarity in composition of each factor spectrum in very disparate regions of the atmosphere, as shown in Fig. 2. Averaging each of the campaigns listed, fuel combustion accounts for 62% of OM (but ranges from 35 to 93%), biogenic and burning emissions from terrestrial vegetation account for 20% (ranging from 0 to 54%), and ocean sources account for 18% (ranging from 0 to 41%).

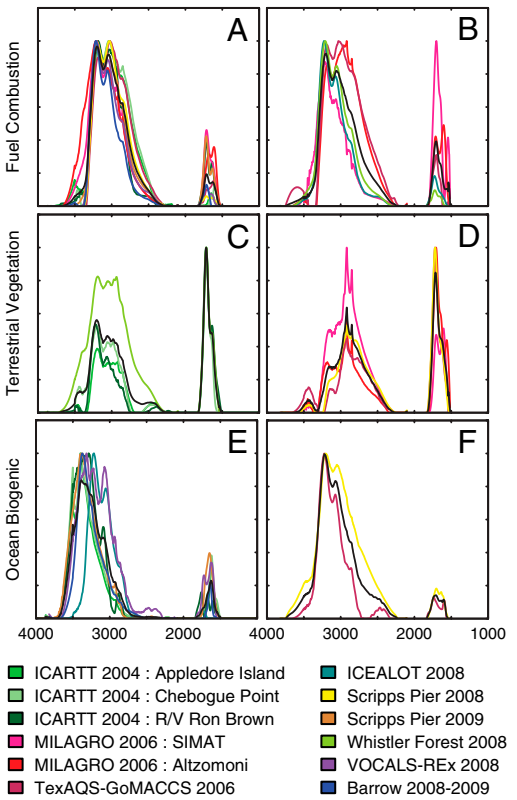

Fig. 2. FTIR spectra of PMF-based factors for fuel combustion (*A*, O/C < 0.4; *B*, O/C > 0.4), terrestrial vegetation (*C*, biogenic; *D*, burning), and ocean biogenic (*E*, O/C > 1; *F*, O/C < 1) sources for the projects with colors given in the legend. The *y* axes are normalized absorbance with arbitrary units.

Fuel Combustion Sources. The observed fuel combustion factors have a mixture of organic functional groups that is dominated by alkane, hydroxyl, and carboxylic acid groups, with small contributions of amine and carbonyl groups in some regions. Combustion factors account for more than 50% of submicron OM in Megacity Initiative: Local and Global Research Operations (MILAGRO), Texas Air Quality Study (TexAQS), and Scripps Pier (La Jolla, California), as well as more than 30% of the International Consortium for Atmospheric Research on Transport and Transformation (ICARTT) studies. The Barrow (Alaska), Whistler, VOCALS, and ICEALOT studies had OM concentrations less than 2 $\mu g\,m^{-3}$ on average and frequently reflected the less proximate or less frequent urban influence at those remote or coastal locations. Fig. 3 shows that the combustion factors from the different locations span a large range of O/C, with the highest O/C combustion factors identified in MILAGRO and TexAQS. The range of O/C measured for most factors is within the 0.25 to 1 range reported previously (26). The correlations of combustion factors with metal markers for primary combustion emissions (S, V, Ni) in TexAQS (and in other campaigns) indicate that these particles may include some primary OM or are formed within 12 h of emission. Such mixtures of primary and secondary components would be correlated in 12-h samples, resulting in combustion factors that could include POA and SOA (16).

The potential contributors to fuel combustion factors are POA and SOA formed from OH oxidation of alkanes (likely from diesel and ship emissions) and aromatics (from gasoline emissions). Though not all SOA products of the OH reactions of aromatics have been identified, they are mostly multifunctional first- and second-generation products that may form oligomers (27–30). Mole fractions of alkane groups in these products are typically <0.3, with the mole fraction of oxygen-containing functional groups (primarily carbonyl, hydroxyl, hydroperoxyl, and nitrate) often approaching 1. Given the large mole fractions of alkane groups (0.49–0.97) and the low mole fractions of carbonyl groups (0.00–0.08) in the combustion factors (Table 1), SOA from aromatic oxidation (which is expected to have lower alkane and higher carbonyl group contributions) is unlikely to account for a substantial fraction of this OM.

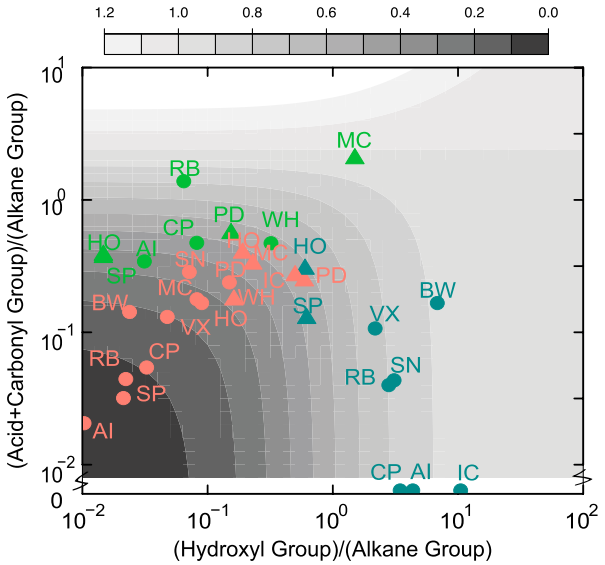

Fig. 3. Molar ratios of organic functional groups in the PMF factors for the atmospheric measurement campaigns listed in Table 1. Labels represent campaign abbreviations given in Table 1, and colors indicate the factor source types with combustion (salmon, circles have O/C < 0.4 and triangles have O/C > 0.4), terrestrial vegetation (jade, circles are biogenic and triangles are burning), and marine (cerulean, circles are O/C > 1 and triangles are O/C > 1), as in Fig. 1. The grayscale background indicates O/C by the scale given in the color bar.

However, this composition is explained by the products of alkane oxidation by OH (23, 24, 31–33). In the NO_x regime (>30 ppt NO, likely for combustion emissions), major first-generation products from reactions of linear alkanes larger than ~C_{10}–C_{15} are ~30% monoalkyl nitrates, ~55% 1,4-hydroxycarbonyls, and ~15% 1,4-hydroxynitrates. In the particle phase, 1,4-hydroxycarbonyls isomerize to cyclic hemiacetals, which then dehydrate to dihydrofurans. The dihydrofurans evaporate and in the atmosphere react primarily with O_3 (34). The SOA-forming products of these O_3 reactions have not been characterized, but are probably similar to those formed from the reaction of similar five-membered ring structures. Studies of the ozonolysis of 1-methyl-cyclopentene and related cyclic alkenes (35) observe that all SOA products of gas-phase reactions are multifunctional and contain at least one carboxylic acid group, with other groups being primarily carboxylic acid, hydroxyl, or carbonyl (as illustrated by Fig. S2).

Examples from the oxidation products of C_{25} and C_{12} alkanes bracket the range of functional group composition observed for most of the combustion factors. Beginning with a C_{25} alkane, which is a reasonable upper bound for chain length of an alkane that under typical atmospheric conditions is largely in the gas phase and has first-generation products that partition almost entirely to the particle phase (23), the SOA should contain (prior to particle-phase reactions) 0.70, 0.55, and 0.45 hydroxyl, carbonyl, and nitrate groups per molecule. Organonitrates may decompose in the atmosphere, probably by hydrolysis to form alcohols (19). The particles would then be 1.15 and 0.55 hydroxyl and carbonyl groups per molecule. Finally, assuming all 1,4-hydroxycarbonyls are converted to dihydrofurans that react with O_3 to form difunctional SOA products with one group being a carboxylic acid and the other being a carboxylic acid, hydroxyl, or carbonyl (in equal amounts ketone and aldehyde) formed with equal probability, the SOA composition becomes 0.73, 0.78, and 0.09 carboxylic acid, hydroxyl, and carbonyl groups per molecule, with no nitrate groups. For a C_{25} compound, the mole fractions are 0.03, 0.03, 0.00, and 0.94 carboxylic acid, hydroxyl, carbonyl, and alkane groups (Table 1). Applying this approach to a C_{12} alkane (for which most of the proposed first-generation products are probably too volatile to form SOA and so react again with OH to form second-generation products via addition of another set of the same functional groups as for a C_{25} compound), this sequence yields mole fractions of 0.12, 0.13, 0.02, and 0.73 for carboxylic acid, hydroxyl, carbonyl, and alkane groups. Additional oxidation of second-generation products in the gas phase or oxidation of smaller alkanes would further increase mole fractions of carboxylic acid, hydroxyl, and carbonyl groups relative to alkane groups, but can also increase fragmentation to form volatile products. Functional group volatility will preferentially enrich particles in carboxylic acid groups over hydroxyl or carbonyl groups.

Using a 24-h average OH concentration of 10^6 molecules cm^{-3} (36), the estimated time scales for oxidation are ~0.8 d and ~0.4 d (1 lifetime) for first-generation C_{12} and C_{25} alkane products and ~1.6 d (2 lifetimes) for second-generation C_{12} alkane products. Although larger alkanes react faster, because their products are less volatile they partition more readily to particles. Considering the ambient variations that affect measured factors —such as the composition of alkane emissions, OH concentrations, and air mass age—the proposed SOA formation from first- and second-generation alkane products provides plausible explanations for a number of interesting characteristics of combustion factors, including (*i*) the range of alkane, hydroxyl, and carboxylic acid group mole fractions, (*ii*) the large mole fractions of alkane groups, (*iii*) the similar or higher mole fractions of carboxylic acid groups compared to hydroxyl groups in most

combustion factors, (*iv*) the almost complete absence of nonacid carbonyl groups, and (*v*) the absence of organonitrate groups.

Terrestrial Biogenic and Burning Vegetation Sources. An important feature of the identified factors is the chemical similarity of the two types of sources associated with terrestrial plants; namely the biogenic emissions of live forests (in Whistler and ICARTT) and the biomass-burning emissions of forest fires and other wood combustion (in TexAQS, MILAGRO, and Scripps Pier 2008). In both the biogenic and burning terrestrial vegetation factors, carbonyl groups are observed in significant quantities, either in addition to or instead of carboxylic acid groups. Similar to combustion factors, the vegetation factors span a large range of O/C in Fig. 3 and are sometimes indistinguishable from combustion on these axes (because acid and carbonyl groups are summed on the *y* axis). The similarity of secondary biogenic particles from live forests with those emitted during forest fires is not surprising, because emissions from burning forests will be mixed with contributions from live trees. Biogenic VOCs associated with forests (such as monoterpenes and isoprene) are also observed in forest fires (37–39), and the similarity of these precursors results in similarities in the resulting SOA. There is also chemical similarity in the primary particles associated with forest and fire emissions because both include cellulose breakdown products (40). Moreover, some biogenic VOCs are expected to have increased emission rates in response to higher temperatures and tissue damage (41), which both accompany tree fires.

The potential contributors of OM to the terrestrial vegetation (live and burning) factors include SOA formed from the oxidation of isoprene and monoterpenes, the dominant biogenic VOC emissions (41). In the atmosphere, isoprene reacts primarily with OH, and laboratory studies indicate the SOA products of the reaction are oligomers with mole fractions of ~0.2–0.4 for alkane groups and ~0.6–0.8 for total hydroxyl, carbonyl, carboxylic acid, organonitrate, hydroperoxyl, and ester groups (42). Monoterpenes react with OH and O_3, and a recent modeling study of α-pinene (the dominant atmospheric monoterpene emission) oxidation under a variety of NO_x conditions estimates that the SOA-forming products have average mole fractions of ~0.76 for alkane groups and ~0.06 each for hydroxyl, carbonyl, and carboxylic acid groups (25), as well as small contributions of "other" groups not identified in these measurements (including ether and aldehyde groups). These contributions are qualitatively similar to the composition for the biogenic factor identified in the remote forested region at Whistler, with mole fractions of alkane, hydroxyl, carbonyl, and carboxylic acid groups of 0.44, 0.25, 0.16, and 0.10, respectively. The mole fractions of oxygen-containing functional groups are all higher than predicted by the model, indicating that the OM in this factor is probably a mixture of SOA formed from first- and second-generation products of monoterpene and possibly isoprene oxidation that is not reflected in the modeled chemistry.

For the three biogenic factors identified in the mixed biogenic-combustion-marine ICARTT region (Chebogue Point, Appledore Island, and R/V *Ronald Brown*), the mole fractions of alkane, hydroxyl, carbonyl, and carboxylic acid groups are 0.31–0.64, 0.02–0.05, 0.22–0.43, and 0.00. Comparing these values with those predicted from monoterpene oxidation modeling (25) suggests that the ambient aerosol is enriched in carbonyl groups and depleted in hydroxyl and carboxylic acid groups relative to predictions. A simple and interesting explanation for this is that the biogenic hydroxyl and carboxylic acid groups reacted in the aerosols during transport downwind of urban areas to form esters (particle-phase reactions are not included in the modeled SOA composition). The carbonyl C = O in ketones and esters absorb in different but overlapping ranges of FTIR, and we lack a set of atmospherically relevant standards to separate their contributions in atmospheric samples. Oligomeric esters have been shown to be a major component in SOA formed from isoprene oxidation (42), and their formation from monoterpene oxidation products is predicted to be thermodynamically favorable under atmospheric conditions (43). If all the predicted hydroxyl and carboxylic acid groups reacted to form esters, then the mole fractions of functional groups in the SOA should be ~0.72 for alkane, ~0.18 for carbonyl, and ~0.00 for hydroxyl and carboxylic acid groups, which agrees reasonably well with the ICARTT biogenic factors. It appears that isoprene oxidation does not contribute significantly to the OM of these three factors, because the expected high mole fractions of hydroxyl and carboxylic acid groups (even after oligomerization) are not observed.

The functional group compositions of the four measured wood-burning factors span approximately the same range as was observed for biogenic factors. The mole fractions of alkane, hydroxyl, carbonyl, and carboxylic acid groups in the wood-burning factors are 0.20–0.68, 0.01–0.30, 0.18–0.39, and 0.02–0.08, indicating that the precursors of SOA in these factors are the same as for biogenic factors. The compositions of the individual campaign factors are more varied, but this range is not surprising given the possible burning conditions and plant species.

Marine Biogenic Sources. Primary emissions of organic-containing particles during bubble bursting at the ocean surface are a significant submicron particle source in coastal and marine regions (17), although a clear signal is sometimes masked by larger urban sources as in TexAQS (16). Marine saccharides could account for global background of up to 0.5 $\mu g\, m^{-3}$ (depending on nearby sea surface wind speeds), an emission category that is omitted in most global models and may account for part of their underprediction of OA mass at remote surface locations (44). Interestingly, the marine POA factors have the highest O/C (as shown in Fig. 3), despite the near absence of carboxylic acid or carbonyl groups.

The high mole fraction of hydroxyl groups (0.30–0.82) in the particles from bubble bursting on the ocean is consistent with the 80% carbohydrate composition of dissolved organic carbon in surface seawater (45). The persistence of these hydroxyl groups in particles is consistent with the low volatility and low expected reactivity of saccharides in the particle phase.

Discussion

In this work we apply the spectral characteristics of organic functional groups measured by FTIR to create a multivariate framework for comparing measured and modeled OM. In the 14 campaign-periods apportioned by source in Fig. 1, fuel combustion sources accounted for more than half of OM in eight studies, terrestrial biogenic and burning vegetation sources for more than a third of OM in four studies, and marine bubble bursting for more than a quarter of OM in seven studies. The highest measured O/C values are found in the marine OM, which is dominated by more than 70% hydroxyl group mass from seawater carbohydrates. The combustion and vegetation factors include a range of O/C for different campaigns. The low O/C combustion factors are significant contributors in campaigns with shipping and diesel emissions; the higher O/C combustion factors are more consistent with the predominantly urban conditions observed in MILAGRO and TexAQS. Interestingly, the ranges of O/C (in Fig. 3) were similar for both biogenic and burning types of terrestrial vegetation sources, with both characterized by substantial fractions of carbonyl groups. Consequently, distinguishing between the combustion, vegetation, and marine sources requires two (or more) independent metrics, such as carbonyl and hydroxyl functional groups [as shown in Fig. 3 and as shown by Decesari et al. (46)], rather than a single metric (such as O/C).

To understand the SOA fraction of the combustion and vegetation sources, we compare the ambient distribution of organic functional groups to SOA products from chambers. The organic

functional group compositions with the lowest O/C values are consistent with an SOA formation model of the oxidation of ~C_{12}–C_{25} alkane precursors (similar to those found in diesel emissions) to form first-generation and multigeneration products, with alkane group mole fractions ranging from ~0.67–0.96 and the remainder being approximately equal or greater amounts of carboxylic acid groups compared to hydroxyl groups. The near absence of carbonyl groups in SOA associated with combustion emissions is explained by the alkane oxidation mechanism, and the absence of organonitrate groups is attributed to hydrolysis in the particle phase. Oxygenated group mole fractions exceeding the upper limit of ~0.25 predicted for alkane oxidation were identified in MILAGRO and TexAQS, which suggests a significant difference in the SOA produced from fuel combustion in these urban centers that requires further study of both atmospheric and chamber organic functional groups.

The nonacid carbonyl groups indicate a link between biogenic and biomass burning OM that is consistent with various mixtures of first- and second-generation SOA products formed from chamber oxidation of monoterpenes and isoprene. Most interesting is the observation that at locations where the biogenic OM is measured downwind of large urban centers (as in ICARTT), the factor composition is depleted in hydroxyl and carboxylic acid groups and enriched in carbonyl groups relative to the composition expected from chamber experiments. This unexpected composition is most simply explained as resulting from the formation of esters via the reaction of hydroxyl and carboxylic acid groups, providing tantalizing field evidence that the formation of esters via condensed-phase reactions is an important source of atmospheric SOA and a possible pathway for oligomerization.

ACKNOWLEDGMENTS. Space, logistical support, and in some cases sample collection were supported by the generosity of collaborators, in particular Patricia Quinn, Tim Bates, Barbara Turpin, Darrel Baumgardner, and Richard Leaitch. The measurement campaigns reported here were supported by the National Science Foundation and the National Oceanic and Atmospheric Administration (including Grants ATM-0744636, ATM-0511772, and ARC-0714052), with the help of many science teams and collaborators. This retrospective comparison was supported by the James S. McDonnell Foundation and BP, as well as ATM-0904203 (L.M.R.) and ATM-0650061 (P.J.Z.).

1. Kroll JH, Seinfeld JH (2008) Chemistry of secondary organic aerosol: formation and evolution of low-volatility organics in the atmosphere. *Atmos Environ* 42:3593–3624.
2. Carlton AG, et al. (2009) A review of secondary organic aerosol (SOA) formation from isoprene. *Atmos Chem Phys* 9:4987–5005.
3. Hallquist M, et al. (2009) The formation, properties and impact of secondary organic aerosol: Current and emerging issues. *Atmos Chem Phys* 9:5155–5236.
4. Paulot F, et al. (2009) Unexpected epoxide formation in the gas-phase photooxidation of isoprene. *Science* 325:730–733.
5. DeGouw J, Jimenez JL (2009) Organic aerosols in the Earth's atmosphere. *Environ Sci Technol* 43:7614–7618.
6. Donahue NM, et al. (2009) Atmospheric organic particulate matter: From smoke to secondary organic aerosol. *Atmos Environ* 43:94–106.
7. Maria SF, et al. (2002) FTIR measurements of functional groups and organic mass in aerosol samples over the Caribbean. *Atmos Environ* 36:5185–5196.
8. Maria SF, et al. (2003) Source signatures of carbon monoxide and organic functional groups in Asian Pacific Regional Aerosol Characterization Experiment (ACE-Asia) submicron aerosol types. *J Geophys Res* 108 10.1029/2003JD003703.
9. Quinn PK, et al. (2004) Aerosol optical properties measured onboard the Ronald H. Brown during ACE Asia as a function of aerosol chemical composition and source region. *J Geophys Res* 109 10.1029/2003JD004010.
10. Maria SF, Russell LM (2005) Organic and inorganic aerosol below-cloud scavenging by suburban New Jersey precipitation. *Atmos Environ* 39:4793–4800.
11. Gilardoni S, et al. (2007) Regional variation of organic functional groups in aerosol particles on four U.S. east coast platforms during the International Consortium for Atmospheric Research on Transport and Transformation 2004 campaign. *J Geophys Res* 112 10.1029/2006JD007737.
12. Bahadur R, et al. (2010) Phenol groups in Northeastern U.S. submicron aerosol particles produced from seawater sources. *Environ Sci Technol* 44:2542–2548 10.1021/es9032277.
13. Gilardoni S, et al. (2009) Characterization of organic ambient aerosol during MIRAGE 2006 on three platforms. *Atmos Chem Phys* 9:5417–5432.
14. Liu S, et al. (2009) Oxygenated organic functional groups and their sources in single and submicron organic particles in MILAGRO 2006 campaign. *Atmos Chem Phys* 9:6849–6863.
15. Day DA, et al. (2009) Organic composition of single and submicron particles in different regions of Western North America and the Eastern Pacific during INTEX-B 2006. *Atmos Chem Phys* 9:5433–5446.
16. Russell LM, et al. (2009) Oxygenated fraction and mass of organic aerosol from direct emission and atmospheric processing measured on the R/V *Ronald Brown* during TEXAQS/GoMACCS 2006. *J Geophys Res* 114:D00F05 10.1029/2008JD011275.
17. Russell LM, et al. (2010) Carbohydrate-like composition of submicron atmospheric particles and their production from ocean bubble bursting. *Proc Nat Acad Sci USA* 107:6652–6657.
18. Hawkins LN, Russell LM (2010) Oxidation of ketone groups in transported biomass burning aerosol from the 2008 Northern California Lightning Series fires. *Atmos Environ* 44:4142–4154 10.1016/j.atmosenv.2010.07.036.
19. Day DA, et al. (2010) Organonitrate group concentrations in submicron particles with high nitrate and organic fractions in coastal Southern California. *Atmos Environ* 44:1970–1979 10.1016/j.atmosenv.2010.02.045.
20. Schwartz RE, et al. (2010) Biogenic oxidized organic functional groups from a mid-mountain forest at Whistler, BC, and their similarities to laboratory chamber products. *Atmos Chem Phys* 10:5075–5088 10.5194/acp-10-5075-2010.
21. Hawkins LN, et al. (2010) Carboxylic acids, sulfates, and organosulfates in processed continental organic aerosol over the Southeast Pacific Ocean during VOCALS-REx 2008. *J Geophys Res* 115:D13201 10.1029/2009JD013276.
22. Shaw PM, et al. (2010) Arctic organic aerosol measurements show seasonal particle sources of spring haze and winter frost flowers. *Geophys Res Lett* 37:L10803 10.1029/2010GL042831.
23. Lim YB, Ziemann PJ (2009) Chemistry of secondary organic aerosol formation from OH radical-initiated reactions of linear, branched, and cyclic alkanes in the presence of NO_x. *Aerosol Sci Technol* 43:604–619.
24. Lim YB, Ziemann PJ (2009) Kinetics of the heterogeneous conversion of 1,4-hydroxycarbonyls to cyclic hemiacetals and dihydrofurans on organic aerosol particles. *Phys Chem Chem Phys* 11:8029–8039.
25. Capouet M, et al. (2008) Modeling aerosol formation in alpha-pinene photo-oxidation experiments. *J Geophys Res* 113(D02308):10.1029/2007JD008995.
26. Aiken AC, et al. (2008) O/C and OM/OC ratios of primary, secondary, and ambient organic aerosols with high-resolution time-of-flight aerosol mass spectrometry. *Environ Sci Technol* 42:4478–4485.
27. Edney EO, et al. (2001) Formation of polyketones in irradiated toluene/propylene/NO_x/air mixtures. *Aerosol Sci Technol* 35:998–1008.
28. Kleindienst TE, et al. (2004) Determination of secondary organic aerosol products from the photooxidation of toluene and their implications in ambient PM2.5. *J Atmos Chem* 47:79–100.
29. Kalberer M, et al. (2004) Identification of polymers as major components of atmospheric organic aerosols. *Science* 303:1659–1662.
30. Johnson D, et al. (2005) Simulating the formation of secondary organic aerosol from the photooxidation of aromatic hydrocarbons. *Environ Chem* 2:35–48.
31. Reisen F, et al. (2005) 1,4-Hydroxycarbonyl products of the OH radical initiated reactions of C_5–C_8 *n*-alkanes in the presence of NO. *Environ Sci Technol* 39:4447–4453.
32. Lim YB, Ziemann PJ (2005) Products and mechanism of secondary organic aerosol formation from reactions of n-alkanes with OH radicals in the presence of NO_x. *Environ Sci Technol* 39:9229–9236.
33. Atkinson R, et al. (2008) Atmospheric chemistry of alkanes: Review and recent developments. *Atmos Environ* 42:5859–5871.
34. Martin P, et al. (2002) Formation and atmospheric reactions of 4,5-dihydro-2-methylfuran. *J Phys Chem A* 106:11492–11501.
35. Gao S, et al. (2004) Low-molecular weight and oligomeric components in secondary organic aerosol from the ozonolysis of cycloalkenes and α-pinene. *J Phys Chem A* 108:10147–10164.
36. Atkinson R, Arey J (2003) Atmospheric degradation of volatile organic compounds. *Chem Rev* 103:4605–4638.
37. Greenberg JP, et al. (1984) Hydrocarbon and carbon monoxide emissions from biomass burning in Brazil. *J Geophys Res* 89:1350–1354.
38. Crutzen PJ, et al. (1985) Tropospheric chemical composition measurements in Brazil during the dry season. *J Atmos Chem* 2:233–256.
39. Karl TG, et al. (2007) The tropical forest and fire emissions experiment: Method evaluation of volatile organic compound emissions measured by PTR-MS, FTIR, and GC from tropical biomass burning. *Atmos Chem Phys* 7:5883–5897.
40. Simoneit BRT, et al. (1999) Levoglucosan, a tracer for cellulose in biomass burning and atmospheric particles. *Atmos Environ* 33:173–182.
41. Guenther A, et al. (1995) A global model of natural volatile organic compound emissions. *J Geophys Res* 100:8873–8892.
42. Surratt JD, et al. (2006) Chemical composition of secondary organic aerosol formed from the photooxidation of isoprene. *J Phys Chem A* 110:9665–9690.
43. Barsanti KC, Pankow JF (2006) Thermodynamics of the formation of atmospheric organic particulate matter by accretion reactions—Part 3: Carboxylic and dicarboxylic acids. *Atmos Environ* 40:6676–6686.
44. Chung SC, Seinfeld JH (2002) Global distribution and climate forcing of carbonaceous aerosols. *J Geophys Res* 107 10.1029/2001JD001397.
45. Aluwihare LI, et al. (1997) A major biopolymeric component to dissolved organic carbon in surface sea water. *Nature* 387:166–169.
46. Decesari S, et al. (2007) Source attribution of water-soluble organic aerosol by nuclear magnetic resonance spectroscopy. *Environ Sci Technol* 41:2479–2484.